

Rapid, At-Sea Detection of Munition Compounds in Coastal Waters Using a Shipboard System

Mario Esposito,* Aaron J. Beck, Maria Martinez-Cabanas, Martha Gledhill, and Eric P. Achterberg



Cite This: *ACS EST Water* 2023, 3, 2890–2898



Read Online

ACCESS |



Metrics & More



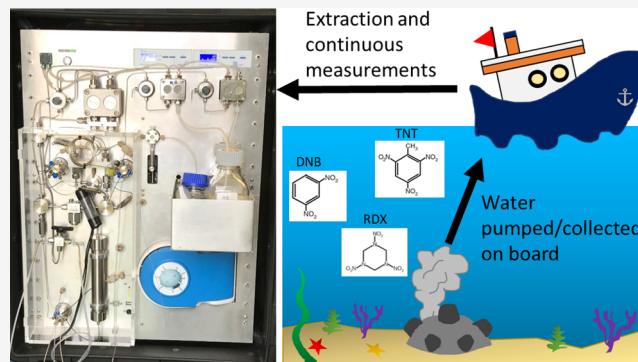
Article Recommendations



Supporting Information

ABSTRACT: Coastal waters are contaminated globally with millions of metric tons of munitions from the two world wars which constitute a potential threat to ecosystems and humans. Laboratory-based chemical methods for the detection of munition compounds (MCs) in seawater typically take weeks to months between sample collection and analysis. The current work details a novel, field-deployable system for rapid (under 10 min) analysis of four common MCs (1,3-dinitrobenzene (DNB), amino-4,6-dinitrotoluene (ADNT), 2,4,6-trinitrotoluene (TNT), hexahydro-1,3,5-trinitro-1,3,5-triazine (RDX)). The system uses a fluidic preconcentration unit with high-performance liquid chromatography (HPLC) and detection by electrospray-ionization mass spectrometry and UV–vis spectroscopy. The fluidic unit comprises two solid-phase extraction (SPE) columns for preconcentration of target MCs from the seawater matrix and allows loading and analysis of two samples simultaneously. Seven SPE resins were tested for extraction efficiency and robustness, with Porapak RDX showing best performance. Chromatographic separation of target MCs was performed using a C8 reversed-phase HPLC column. Limits of detection (LODs) were 3.7, 1.8, 3.6, and 10.7 ng L⁻¹ for DNB, ADNT, TNT, and RDX, respectively. The system's analytical performance and automated data processing procedure were demonstrated in the Baltic Sea.

KEYWORDS: *Porapak RDX, 2,4,6-trinitrotoluene, amino-dinitrotoluene, 1,3-dinitrobenzene, hexahydro-1,3,5-trinitro-1,3,5-triazine, on-site measurements*



INTRODUCTION

Large quantities of unexploded ordnance were disposed in coastal waters globally during and after the wars in the last century. Sea disposal of conventional and chemical munitions has been prohibited since 1972,¹ and a number of munition clearance operations have been performed since then.² However, millions of metric tons of munitions can be found at munition dumping sites in coastal waters and constitute a potential threat to ecosystems and humans. Many decades have passed since most munitions were dumped, and corrosion of metal housings and casings is increasing the risk of contaminant release and the hazard of self-detonation.³ The safety of offshore activities including installation of wind farms and underwater cables as well as fishing, shipping, and tourism is therefore endangered. The leakage of munition compounds (MCs) from corroding shells into surrounding waters and sediments may have detrimental impacts on marine ecosystems.⁴ Nitro-aromatic compounds (e.g., 2,4,6-trinitrotoluene, TNT; 1,3-dinitrobenzene, DNB) and nitramines (e.g., hexahydro-1,3,5-trinitro-1,3,5-triazine, RDX), typically present in conventional munitions, are known for their toxicity and carcinogenicity with evidence of chronic detrimental effects on

aquatic biota living in proximity of dumpsites and potentially including organisms caught for human consumption.^{5–7}

Munitions search and clearance activities generally employ geophysical techniques. These allow mapping of local distributions of munition shells on and in the seabed, but lack specificity. For example, magnetometers and sub-bottom profilers can identify magnetic and dense objects on and below the seafloor. The objects can be munition shells, but also marine litter, leading to a potentially high number of false positives.⁸ Sidescan sonars and multibeam echo sounders provide images of objects on the seafloor, but algal overgrowth and poor preservation of munition housings can make them difficult to distinguish from rocks or garbage. High-resolution images obtained with optical systems or direct video inspection by remotely operated vehicle (ROV) allow us to accurately identify the objects on the seafloor. However, these techniques

Received: March 1, 2023

Revised: July 25, 2023

Accepted: July 26, 2023

Published: August 8, 2023



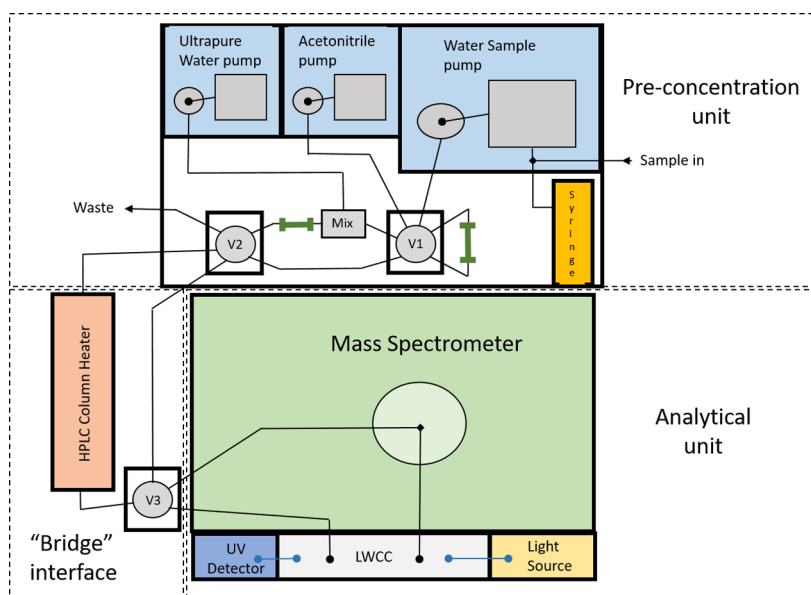


Figure 1. Schematic diagram of the system. Preconcentration unit: two multiport switching valves (V1, V2) direct fluid from three HPLC pumps, two solid-phase extraction (SPE) columns, and one syringe pump for standard addition. Bridge interface: one 6-port switching valve (V3) and a C8 reversed-phase HPLC column with heater. Analytical unit: compact electrospray ion source mass spectrometer and liquid waveguide capillary cell (LWCC) coupled with light source and ultraviolet (UV) detector.

are limited to individual objects, favorable water conditions, and require expert guidance. Furthermore, the use of these techniques is typically more challenging in deep waters, leading to higher risk scores for deep water hazards.⁹

Leakages of MCs and formation of MC plumes in the water column are a consequence of openings in the munition shells due to corrosion,¹⁰ and chemical detection has been identified as a viable ordnance tracing tool. The application of analytical chemical techniques would allow for unequivocal detection of the presence of munition objects requiring clearance, particularly at sites where geophysical techniques may fail or provide ambiguous information. Moreover, the chemical detection of MCs can facilitate the identification of the type of munition present on the seafloor.

Laboratory methods for MCs typically use a combination of traditional techniques like solvent extraction followed by high-performance liquid chromatography (HPLC) separation and UV–Vis detection, to analyze dissolved MCs at concentration levels of $\mu\text{g L}^{-1}$.¹¹ Recently, mass spectrometry (MS) techniques have been reported for MC analysis, enhancing sensitivity and selectivity of the detection. Only a few of these methods have been applied to marine samples. Gledhill and co-workers¹² have recently developed a novel method for the detection and unequivocal identification of 15 MCs in seawater. The method is based on solid-phase extraction and UHPLC-MS detection and has been validated at munition-contaminated sites in the Baltic Sea and is highly sensitive for most of the prevalent MCs. This laboratory method for munition detection is however expensive and time- and labor-intensive employing weeks to months from sample collection, transport, storage, preparation, and analysis to results.

Several direct sensing techniques for MCs have been reported, including square-wave voltammetry,¹³ neutron analysis,¹⁴ Raman spectroscopy,¹⁵ or amplifying polymer sensors.¹⁶ The direct chemical sensing of MCs is cost-effective and provides rapid in situ results. A highly selective and ultrasensitive surface-enhanced Raman spectroscopy sensor

was able to successfully detect 0.4 ng L^{-1} TNT dissolved in water,¹⁷ while detection of ammonium nitrate (NH_4NO_3), pentaerythritol tetranitrate (PETN), TNT, high melting explosive (HMX), and RDX dissolved in solvent/water solution at concentrations below 1 mg L^{-1} was reported for deep UV resonance Raman spectroscopy technique.¹⁸ However, in situ detection of MCs in seawater at concentrations present at munition dumping sites (ng L^{-1}) has not been reported so far. Moreover, some of the in situ detection methods suffer from interferences by nonexplosive organic compounds and only focus on the detection of single MCs, which can lead to false-negative results when munitions contain nontarget explosives.

Therefore, analytical systems capable of measuring multiple MCs in seawater at nanomolar levels and within short times are required. Innovative approaches able to provide on-site feedback would facilitate both monitoring and commercial or military munition clearance operations at marine dumpsites. Here, we describe the development of a field-deployable analytical system for direct on-site chemical identification and quantification of dissolved DNB, TNT, ADNT, and RDX in seawater. Preconcentrated MCs from seawater are detected with a compact electrospray-ionization MS (ESI-MS) and UV setup for dual detection in under 10 min. The system performance was demonstrated at sea during a research campaign in the Baltic Sea.

EXPERIMENTAL SECTION

Reagents and Standards. Certified stock standards (1 mg L^{-1}) of hexahydro-1,3,5-trinitro-1,3,5-triazine (RDX), 2,4,6-trinitrotoluene (TNT), 2-amino-4,6-dinitrotoluene (2-ADNT), 4-amino-2,6-dinitrotoluene (4-ADNT), and 1,3-dinitrobenzene (DNB) were obtained from Accu Standards (New Haven, CT). Custom mixed analytical standard solutions were prepared from dilutions of single standards in 1:1 (v/v) methanol (MeOH)/acetonitrile (ACN), both LCMS grade (Optima, Fisher Scientific). Isotopically labeled TNT

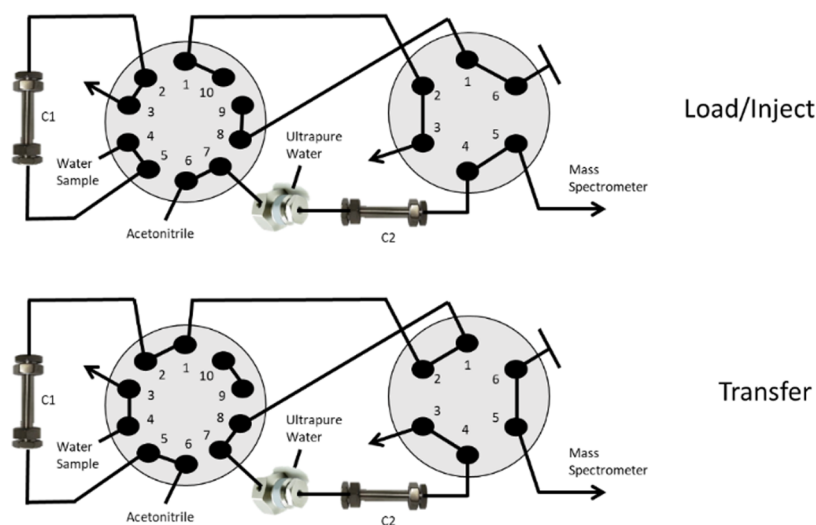


Figure 2. Novel elution–dilution two-column setup.

($^{13}\text{C}^{15}\text{N}$ -2,4,6-trinitrotoluene, hTNT) standard (1 g L^{-1}) was obtained from Cambridge Isotopes (LGC Standards, Germany) and used as internal standard following dilution in 1:1 (v/v) MeOH/ACN. Stock standards and analytical standards were stored in 1.5 mL amber glass (Omnilab) and 10 mL brown glass (Rotilabo) vials, respectively, at $-20\text{ }^{\circ}\text{C}$ and in the dark to prevent degradation and retard evaporation. High-purity water (MQ, $18.2\text{ M}\Omega\text{ cm}$, Milli-Q, Millipore) was used throughout, and $0.2\text{ }\mu\text{m}$ filtered (AcroPak capsules, Pall Corporation) natural seawater from Kiel fjord (Germany) was used to test for organic matter and other potential sample matrix interferences. Solutions of 15 mM HPLC-grade sodium formate (Sigma-Aldrich) prepared in 50:50 (v/v) high-purity water/2-propanol were used to calibrate the mass spectrometer in the mass range between 50 and $800\text{ }m/z$ in both positive and negative ionization modes.

Solid-Phase Extraction. Solid-phase extraction (SPE) for both qualitative and quantitative determination of MCs in aqueous samples was performed on 7 commercially available solid sorbents (Table S1). Resins were packed into modular HPLC columns of different sizes ($50 \times 4.6\text{ mm}$, $50 \times 2.1\text{ mm}$, $30 \times 2.1\text{ mm}$, and $10 \times 2.1\text{ mm}$, length \times internal diameter (I.D.)) to test for absorption and extraction performance. Prior to filling, the sorbents were washed with 100% MeOH, followed by rinsing (20 mL min^{-1} for at least 2 min) with high-purity water after packing. A continuous flow setup was used to perform extraction of MCs and subsequent elution of the analytes loaded on the column (Figure S1). The target analytes were eluted from the columns using ACN as solvent.

Instrument Hardware Components and Workflow. The system was installed in two military-grade shock-protected electronic rack boxes to allow for portability and easy field or shipboard deployment. The full device comprised two main modules: a preconcentration system and an analytical unit (Figure 1).

The preconcentration module employed a novel elution–dilution two-column setup to achieve up to a 5000-fold sample concentration factor within a period of 10 min (Figure 2).

The module comprised two multiport switching valves (Valco Instruments Co., Inc.) and three HPLC pumps (two Azura P4.1S and one Azura P2.1L, Knauer GmbH). The sample (usually 1 L) was pumped over the first (C1 or

“sample”) column using the high-flow (500 mL min^{-1} max) HPLC pump. The sample column was a $50 \times 4.6\text{ mm}$ I.D. stainless steel (SS) HPLC column packed with SPE resin. The analytes adsorbed on the resin were then eluted from C1 with ACN using the low-flow (10 mL min^{-1} max) HPLC pump, diluted online with high-purity water pumped by a second low-flow HPLC pump, and preconcentrated on a second (C2 or “analytical”) column. The ACN HPLC pump was then used to elute the analytes from C2 and direct them toward the analytical detection unit. The analytical column was smaller ($30 \times 2.1\text{ mm}$ I.D.) than C1, allowing further preconcentration of the target analytes to produce sharp and regular peaks. The dual-column setup also provided loading and analysis of two different samples simultaneously allowing for a higher sampling frequency. Within the preconcentration unit, a 1 mL syringe pump (Cavro XCalibur, Tecan) equipped with a 3-port distribution valve was used to deliver either internal standard or calibration solutions into the sample inlet line.

Preconcentrated samples were carried to the analytical module via a “bridge” interface. The unit consisted of a 2-position 6-port switching valve (Rheodyne, IDEX Health & Science), and a custom-made compact column heater (precision $\pm 0.05\text{ }^{\circ}\text{C}$) chamber hosting a $150 \times 3.9\text{ mm}$ C8 reversed-phase ($4\text{ }\mu\text{m}$ particle size) HPLC column (NovaPak) for chromatographic separation of MCs. Interfering nontarget organic compounds eluted within the first 2 min from the HPLC column were diverted to waste via the switching valve. The valve was then switched, and the column effluent containing the target compounds was diverted to the analytical unit.

The analytical module consisted of a compact MS (4500 MiD, Microsaic Systems) and an integrated UV setup for dual detection. The 4500 MiD employs a micro-ESI source to form gas-phase analyte ions that are guided under vacuum through a series of ions optics and finally focused on a micro-engineered quadrupole mass analyzer according to their mass-to-charge (m/z) ratios. The ESI was operated in negative ionization mode with a tip voltage offset of -750 V . The MS was run either in scan or selected ion monitoring (SIM) mode. In SIM mode, masses $168.0\text{ }m/z$, $196.1\text{ }m/z$, $226.1\text{ }m/z$, $236.1\text{ }m/z$, and $257.0 + 259.0\text{ }m/z$ were used for the quantification of DNB, ADNT, TNT, hTNT, and RDX, respectively. Nitrogen

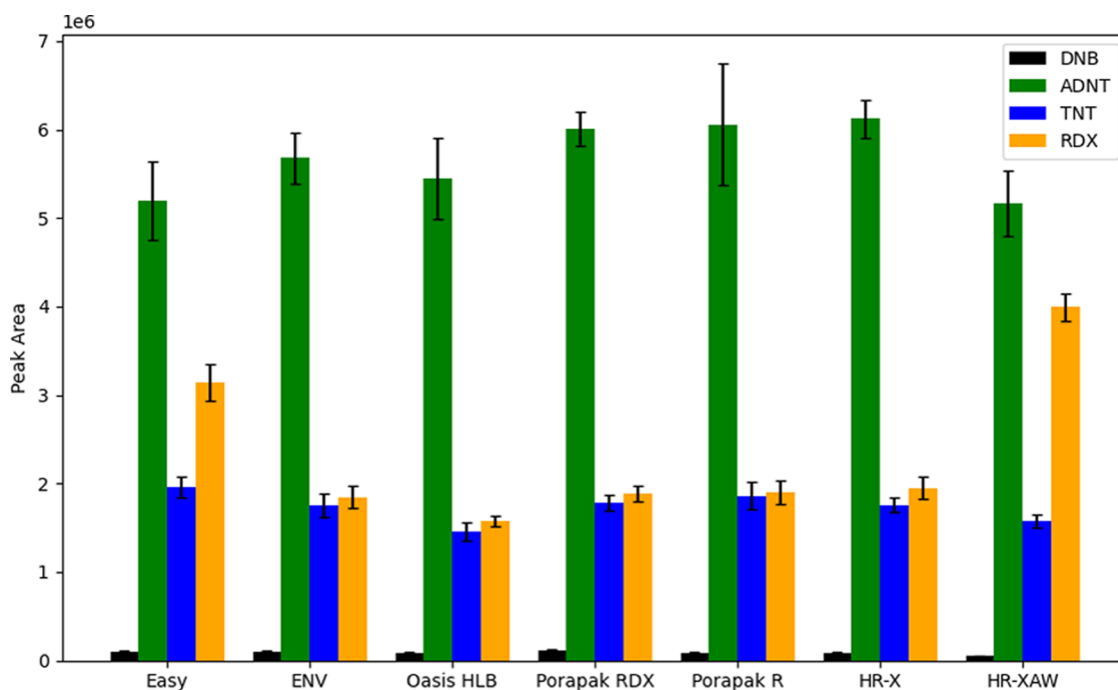


Figure 3. Comparison of peak areas of munition compounds eluted from different resins. Error bars represent the standard deviation of 20 replicates.

gas (2.5 L min^{-1}) was provided by a high-purity N_2 generator (Solaris 10, Peak Scientific). The 1 mL min^{-1} sample influent flowing from the “bridge” interface was split, with $1 \mu\text{L min}^{-1}$ entering the MS and the remaining $999 \mu\text{L min}^{-1}$ routed into the UV detection unit. The UV module used a compact detector (USB400, Ocean Optics) to monitor the sample absorbance at 254 nm in a 1-m-long liquid waveguide capillary cell (LWCC, World Precision Instruments). A halogen-deuterium lamp (DT-MINI-2-GS, Ocean Optics) was used as a light source, and two SMA-terminated, 400 μm diameter fiber-optic cables (Ocean Insight) transmitted light to and from the LWCC.

Software and System Control. The 4500 MiD unit has an embedded software interface (Masscape v. 3.3.1) to control all features of the instrument, including data acquisition and analysis. Masscape was used to perform periodic mass calibrations and to monitor vacuum and spray current during runs. The UV spectrometer was controlled by OceanView software (v. 1.6.5) that allows for monitoring and acquisition of absorbance data at specific wavelengths. OceanView was used to create a time-acquisition experiment for saving absorbance data to an ASCII file and update dark and reference spectra prior to each instrument start-up. Pumps and valves are controlled either manually by using the function keys on the front of the device and controller, respectively, or externally with a host control system by means of the communication interface RS-232 port. Following appropriate serial port configuration settings, the latter option was chosen to remotely operate all of the components including the 4500 MiD (via socket connection) by using a custom-made user-friendly graphical interface written in Python (v 3.8). Run sequences incorporated user-defined number of samples, loading times, flow rates, and addition of standards. The program also allowed us to have full control of the various hardware components. Continuous monitoring of the back-pressure from the HPLC pumps, valve position, descriptions of

the running status as text, and graphical representation of real-time data acquisition were included.

RESULTS AND DISCUSSION

Extraction Efficiency, Recovery, and Reuse. The optimal SPE sorbent for MC preconcentration and matrix removal was chosen based on target compound extraction efficiency, resin regeneration, and robustness, ability to withstand high flow rates and high pressures, and elution performance including speed and solvent concentrations.

Commercial SPE resins were purchased pre-packed in plastic cartridges and re-packed into different SS HPLC columns. Approximately 220 mg of resin material was re-packed into $50 \times 2.1 \text{ mm}$ I.D. columns connected to a 6-port switching valve (Figure S1). For each resin, 20 replicates of a mixed standard solution ($10 \mu\text{g L}^{-1}$) of MCs (DNB, ADNT, TNT, and RDX) prepared in high-purity water were pumped through the column. The pump flow rate was set to 10 mL min^{-1} with a loading time of 1 min per sample. The loaded analytes (100 ng) were eluted from the resin with 80% ACN. The eluted samples were diluted in line with high-purity water to 40% ACN during the injections (5 min) into the MS for improved ionization during the analysis. The extraction efficiency of each resin was evaluated according to the peak area of each compound monitored during the MS analysis in scan mode (Figure 3).

The resins showed comparable extractions of both the nitroaromatic compounds (TNT, DNB, ADNT) and the nitramide, RDX. The variations in peak area for the tested resins were below 10% for DNB, ADNT, and TNT, but it was as high as 38% for RDX. The unusually high RDX areas determined for HR-XAW were apparently due to a higher background intensity measured at 257.0 m/z compared to the other resins. The same interference was observed for samples extracted from the EASY resin, which is a combination of HR-X and HR-XAW. Interferences caused by the release of contaminants

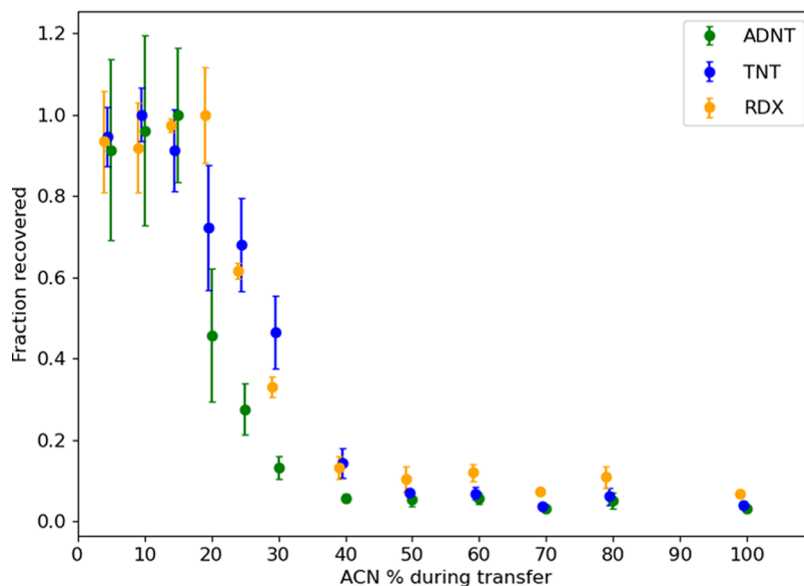


Figure 4. Effect of acetonitrile (ACN) concentration on the recovery of muniton compounds from aqueous solution on Porapak RDX resin. Error bars represent the standard deviation of at least three replicates (between 3 and 10). RDX and TNT data points are shifted by -1 and -0.5 , respectively, on the x -axis to avoid overlapping.

from the interior of the resins were previously reported and attributed to either degradation or swelling and reorientation of the polymer matrix.¹⁹ All tested resins showed good reproducibility among the 20 replicates with the best reproducibility ($<5\%$) obtained for ENV, Porapak RDX, and HR-X resins.

Resin performance was then tested under high flow and pressure conditions. Higher loading flow rates should lead to higher concentration factors in shorter times. The aim was to preconcentrate between 100 and 1000 mL of sample in less than 10 min with no loss in extraction efficiency of the selected MCs. The HPLC sample pump was able to deliver flow rates of up to 500 mL min^{-1} with an operating pressure threshold set to 100 bar. The effect of increasing flow rates on the resin performance was tested both by loading increasing amounts of standards (100, 500, and 1000 ng) and by loading a fixed amount (100 ng) of mixed standard with reduced loading times (Figure S2). Different backpressure values were observed for samples loaded onto the different resins, apparently as a result of differing resin mesh size. Backpressure values above 100 bar were observed for columns packed with the two smallest particle size sorbents (HLB and HR-X, Table S1), so peak areas at flow rates of 100 mL min^{-1} were not available for these resins. As pressures were consistently high on HLB and HR-X sorbents, the resins were considered unsuitable for the system and excluded from further tests. Samples loaded onto the largest particle size resin (Porapak R, Table S1) exhibited pressure values below the pump threshold, but the peak was on average 30% smaller compared to the other resins. Larger-grain-size resin may require longer contact time to allow full extraction of MCs from the aqueous matrix. As the extraction efficiency of Porapak R was poor, this resin was also excluded from further tests. Among the resins with intermediate particle sizes (EASY and HR-XAW, Table S1), different chemical behaviors were observed. The extraction performances of the EASY and HR-XAW resins were inconsistent for TNT and RDX. It appeared that with an increasing contact time between the sample and resin, the extraction efficiency for TNT

decreased and RDX interferences increased. TNT adsorption was suppressed at a higher flow rate, with clear decreases in peak areas despite the higher amounts loaded. The EASY and HR-XAW resins were therefore omitted in further tests because of inconsistent TNT extraction and high RDX backgrounds. The resins ENV and Porapak RDX provided stable results, with variations in peak areas calculated from 100 ng of TNT and RDX loaded at different flow rates ($10\text{--}100 \text{ mL min}^{-1}$) lower than 10%. Surprisingly, the extraction of TNT and RDX on these resins was poor when the highest sample amount (1000 ng) was loaded on the columns. The values of the calculated peak areas were about 40% lower than that extrapolated at lower loading values. It is likely that resin capacity was saturated at high loading values. Environmental dissolved MC concentrations in the Baltic Sea close to muniton dumpsites are in the range of $0.2\text{--}200 \text{ ng L}^{-1}$,^{7,20} and resin saturation is unlikely to affect the measurements in natural water samples. Therefore, the ENV and Porapak RDX were selected as the best resins for further optimization.

Extraction Capacity and Amount of Resin. In order to test the loading capacity of the resins, about 24 mg of Bond Elut ENV and Porapak RDX sorbents were separately packed into two sets of three $10 \times 2.1 \text{ mm I.D.}$ columns (C1–C3). An additional $50 \times 2.1 \text{ mm I.D.}$ column (C4) containing about 10 times the amount of resin (220 mg) was also prepared for each of the resins. A mixed standard solution ($10 \mu\text{g L}^{-1}$ of ADNT, TNT, and RDX; $100 \mu\text{g L}^{-1}$ for DNB due to poor ionization) was loaded on the four columns connected in series (Figure S3) at a flow rate of 10 mL min^{-1} for 2 min. Each column was then disconnected and sequentially eluted and analyzed in the following order: C1, C4, C3, and C2 to test resin extraction efficiency. Four replicate runs were performed with an additional fifth run in which C1 was replaced by C4 both during loading and analysis (Figure S4). The extraction capacity of the selected MCs (DNB, ADNT, TNT, and RDX) for the two resins was comparable with average total variations in peak areas below 20 and 15% for ENV and Porapak RDX, respectively, for the same column type analyzed

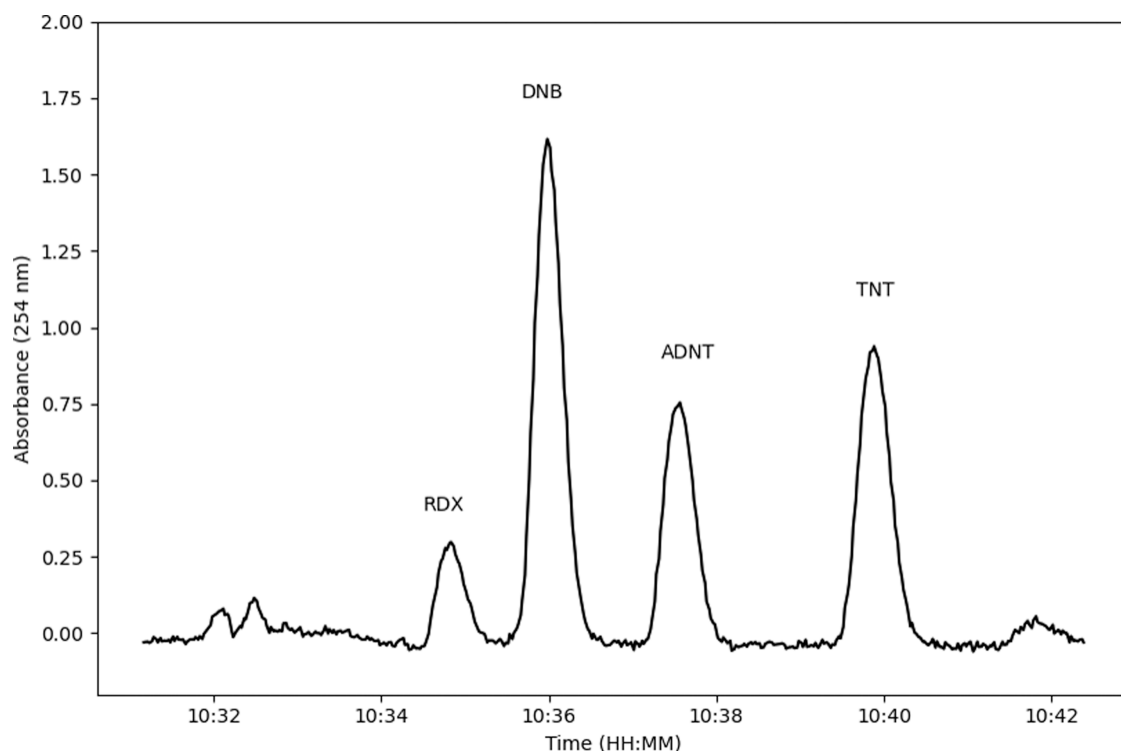


Figure 5. Absorbance scan at 254 nm showing chromatographic separation on a C8 column following extraction and elution using Porapak RDX resin of 20 ng of munition compounds (RDX, DNB, ADNT, and TNT) diluted in high-purity water and carried by a 36% acetonitrile mobile phase. The injection volume was 200 μL , and the HPLC column was kept at 40 $^{\circ}\text{C}$.

in each set of runs. As expected, 24 mg of resin was not sufficient to extract the full amount of MCs contained in the loaded aqueous solutions (200 ng) and at least 3 times (C1–C3) the amount of resin (about 72 mg) was required to recover on average 50% of the dissolved compounds. On the other hand, when C4 was used as the main loading column in run 5, no peaks appeared from the successive analysis of the connected columns (C1–C3) and the resulting peak areas for the extracted MCs on C4 were within 20% of the sum of the areas C1–C3 in the previous tests. Assuming that extraction capacity is proportional to the amount of resin, at the load flow rate (10 mL min^{-1}), ~ 250 and 380 ng of MCs could be retained on 200 mg of ENV and Porapak RDX sorbents, respectively. The higher extraction capacity for Porapak RDX compared to ENV was clear from the MS signal as the scans obtained from the samples extracted with the Porapak RDX resin showed better signal-to-noise ratios compared to the ones extracted with the ENV (Figure S4). As signal intensities up to 1.5 times higher (except for DNB) were observed, the Porapak RDX sorbent was considered for further tests.

Solvent Elution and Analyte Transfer to a Second Column. The two-column elution–dilution approach relies on a sufficiently high concentration of solvent to elute the analytes from one column and a sufficiently low concentration of solvent to allow full extraction of the eluted-diluted analytes on the second column. A mixed standard solution (10 $\mu\text{g L}^{-1}$) of the MCs was prepared in high-purity water and loaded on the sample column (C1) at 10 mL min^{-1} for 4 min (i.e., 400 ng of the target compounds). The compounds were eluted from C1 using 80% ACN and then diluted with high-purity water to ACN concentrations down to 5% and transferred to the analytical column (C2). Each sample was eluted from C2 and carried to the MS using 80% ACN at 1 mL min^{-1} . The use of

100% ACN both during the transfer and elution was also investigated. A sharp decrease in MC recovery occurred when ACN concentrations above 40% were used to transfer the sample from C1 to C2 (Figure 4). At solvent concentrations below 20%, the recovery of MC was above 80%, while no adsorption was observed at ACN concentrations above 60%. An ACN/water mixture of 80/20 was chosen to elute target analytes from C1, and a 5% ACN concentration was chosen for quantitative sorption on C2.

Analytical Performances. HPLC Column Separation and UV Detection. Hyphenation of UV systems with HPLC is a common procedure for the analysis of MCs as the majority of these compounds absorb light in the UV region (190–400 nm). Variable-wavelength or diode array detectors can be used, although determination at 254 nm is often chosen as specified in Method 8330,¹¹ and because of the low incidence of interference at this wavelength.²¹ The preconcentration system uses three HPLC pumps for the propulsion of sample, ACN, and high-purity water. Solutions from the HPLC pumps are routed through the two high-pressure SPE columns for extraction and analysis via the two switching valves. The sample loaded on C1 is eluted using ACN 80% into a 1 mL loop. From the loop, the sample is then transferred to the analytical column (C2) with the addition of high-purity water using a final ACN concentration of $\sim 5\%$. Analytes are eluted from C2 with 80% ACN into a 200 μL loop. The concentrated sample is then directed to the analytical module.

Mass spectrometry does not require separation of target compounds, but initial field tests showed major interferences from natural organic compounds, present at enhanced concentrations in coastal waters, due to the low mass resolution of the compact MS. Additionally, ionization of DNB in the ESI source was poor, in contrast to sensitive

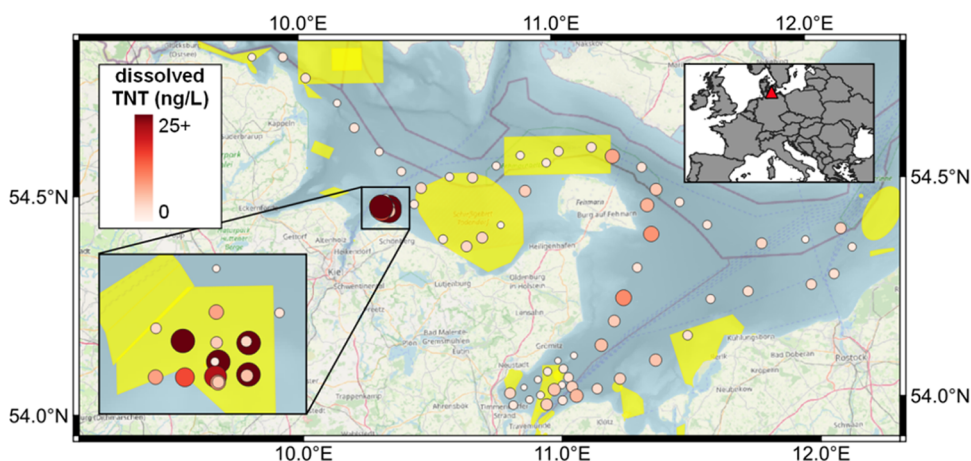


Figure 6. Dissolved TNT in bottom water throughout the southwest Baltic Sea. Symbol size and shading are proportional to TNT concentration. Discrete samples were collected from the Niskin rosette and measured shipboard immediately after collection. The color inset shows an expanded view of samples in Kolberger Heide, and the grayscale inset shows the study location in Europe marked with a red triangle. Yellow polygons indicate regions with munitions dumpsites or known munitions contamination (from amucad.org).²⁸ Map drawn using QGIS version 3.22.4, with basemap from OpenStreetMap and bathymetry shading from GEBCO Compilation Group (2022).²⁹

detection by UV spectrometry. Based on literature reports, four columns operating at typical HPLC conditions (<400 bar) were tested (Table S2). The C8 column was chosen as the most appropriate for the system. Due to the low retention time of the nonpolar compounds in the C8 column, clear separation of the target compounds was obtained in less than 8 min at a flow rate of 1 mL min⁻¹ using ACN (36%) and a column temperature of 40 °C (Figure 5). Chromatographic separation was performed before injection into the MS and UV detector modules to separate target analytes from nontarget organic matter and one another.

Automation of Data Transfer, Peak Integration, and Data Processing. The complex timing of sample loading, solution pumping, and valve switching was carefully calibrated and automatically controlled by a custom-made graphical interface written in Python (3.9). Besides hardware control, the software was used for real-time data acquisition, visualization, and processing. Mass monitoring parameters were set and acquisition started remotely. MS data were remotely retrieved and saved into a text file. Data from the UV spectrometer were also retrieved in real time and added to the same text file.

The presence of UV-absorbing nontarget compounds may interfere with the determination of absorption maxima at specific wavelengths (i.e., 254 nm), particularly in coastal waters with high concentrations of chromophoric dissolved organic matter (CDOM). Excessive residual organic matter was also found to hinder the MS interface and the UV flow cell, leading to long hysteresis and UV signal saturation. As many nontarget compounds eluted first from the chromatographic column, the first 2 min of the injection were diverted to waste by the third switching valve, which greatly improved the signal and reduced interferences. Even with the diverter, the UV signal was still partially affected by residual and variable organic matter content. Spectral slope values for narrow ranges ($S_{275-295}$, $S_{290-350}$, $S_{350-400}$) have been used elsewhere to characterize the nature of DOM in natural waters.^{22,23} This technique was used to compensate for a variable CDOM content, with the slope of absorbance between 275 and 295 nm ($S_{275-295}$) used to compute absorbance at 254 nm

$$A_{254(\text{corrected})} = A_{254(\text{measured})} - A_{\text{CDOM}} \quad (1)$$

$$A_{\text{CDOM}} = S_{275-295} \times 254 \quad (2)$$

The corrected absorbance at 254 nm was then plotted in real time together with the target mass intensities retrieved from the MS. The extracted ion chromatograms were smoothed using a Savitzky–Golay filter and baseline-corrected using a 2nd-degree polynomial fit and Zhang fit algorithms with Python package BaselineRemoval v 0.1.3²⁴ for MS and UV data series, respectively. For each of the monitored masses, peaks were determined as the highest intensity point within pre-set retention time windows, while peak integration was performed according to user-determined peak widths (Figure S5). Peak area was used to quantify TNT, ADNT, and RDX, and peak height was used to quantify DNB.

UV and MS Detector Calibrations. Measurement accuracy and precision were determined using external and internal standards. Natural seawater contains substances that can affect both preconcentration and detection of the target compounds. Therefore, an internal standard was used to compensate for these effects. Moreover, as certified reference material for dissolved MCs is currently not available, the addition of isotopically labeled TNT to natural samples greatly improved the confidence of the analysis. An integrated syringe pump was used to sequentially inject appropriate solution volumes into the sample stream during loading onto the SPE column. The analytical performance of the system was tested for linear response using a standard calibration series. Up to 20 ng of TNT and ADNT, 25 ng of hTNT and DNB, and 100 ng of RDX (variable masses due to differing sensitivity of detection) were injected during the loading phase into a stream of 500 mL of natural seawater (Figure S6). The calibration plots showed good linearity ($R > 0.99$) over the tested ranges with calculated limits of detection (LOD) down to 3.7, 1.8, 3.6, and 10.7 ng L⁻¹ for DNB, ADNT, TNT, and RDX, respectively. The LODs were estimated based on the obtained calibration curves for each of the MCs analyzed as 3 times the standard deviation of the y -intercepts over the slopes. The calibration coefficients from the linear regression plots and sample volumes were used to determine the final concentrations of MCs in unknown seawater samples. The recovery of the target compounds in

natural seawater can vary according to the quantity and quality of dissolved organic matter. The hTNT peak area was used to monitor the recovery of TNT and other compounds allowing for near real-time evaluation and correction of the data outputs.

Application to Natural Seawater Samples. The prototype system was tested in the field in October 2021 during a research cruise in the Baltic Sea on RV Alkor. Numerous conventional munition dumpsites are present in the Baltic Sea, and the Kolberger Heide dumpsite in Kiel Bay is one of the largest with an area of ca. 15 km² containing ~24 000 tonnes of munitions such as sea mines, ground mines, and torpedo heads.²⁵ Kolberger Heide is located about 2 km offshore in water depths between 5 and 20 m. A total number of 81 stations throughout the southwest Baltic Sea were sampled using a Niskin bottle rosette, with a particular focus on the Kolberger Heide dumpsite. Dissolved MC concentrations in the deepest samples (~2 m above seafloor) were measured on board immediately after collection (Figure 6). Dissolved TNT concentrations ranged between 0.5 and 51.5 ng L⁻¹ in the study area, with a median concentration of 3 ng L⁻¹. These levels are consistent with previous measurements in this region.^{26,27} The concentration of the other MCs in the Baltic Sea was below the LODs of the current system. Substantial spatial variability was evident at the Kolberger Heide dumpsite (Figure 6, inset), but a third of the 19 samples measured at the site had TNT concentrations above 10 ng L⁻¹ (median 7.5 ng L⁻¹), compared with only one sample above that threshold (10.3 ng L⁻¹) in the remainder of the study region (median 2.8 ng L⁻¹).

CONCLUSIONS

A novel, field-deployable system was developed and optimized for the detection of four dissolved MCs (DNB, ADNT, TNT, and RDX) in seawater. The novel dual-column preconcentration scheme provided an up to 5000-fold sample concentration factor with simultaneous extraction and analysis of MCs. The combination of a two-way switching valve and a C8 reversed-phase HPLC column allowed for the removal of unwanted nontarget organic compounds and reproducible chromatographic separation of MCs, respectively. The system performance was demonstrated during a research campaign in the Baltic Sea with successful detection and quantification of TNT in natural seawater. The fast analysis time (less than 10 min), low LODs (in the nanomolar range), and automated operation make the system ideal for on-site monitoring, search, and identification of common conventional MCs in seawater. The instrument can support munition clearance operations, and the ability to detect and quantify dissolved MCs can help to monitor contaminant release during clearance operations. The system has further potential applications for monitoring unremediated contaminated dumpsites, improving the safety of marine operations during ordnance clearance, and reducing costs associated with munition identification and removal during commercial offshore development.

ASSOCIATED CONTENT

Supporting Information

The Supporting Information is available free of charge at <https://pubs.acs.org/doi/10.1021/acsestwater.3c00096>.

List of sorbents tested, schematics of continuous flow setup and valve configuration, comparisons of extraction

efficiencies under variable flow rates, concentrations and amount of resin, mass spectrometry and UV data processing procedures, calibration runs, determination of optimal HPLC column, and concentrations of TNT at each sampling location (PDF)

AUTHOR INFORMATION

Corresponding Author

Mario Esposito – GEOMAR Helmholtz Centre for Ocean Research Kiel, 24148 Kiel, Germany; orcid.org/0000-0002-2575-7814; Email: mesposito@geomar.de

Authors

Aaron J. Beck – GEOMAR Helmholtz Centre for Ocean Research Kiel, 24148 Kiel, Germany; orcid.org/0000-0001-9669-0138

Maria Martinez-Cabanas – GEOMAR Helmholtz Centre for Ocean Research Kiel, 24148 Kiel, Germany; Departamento de Química and CICA – Centro Interdisciplinar de Química e Biología, Universidad da Coruña, 15008 A Coruña, Spain

Martha Gledhill – GEOMAR Helmholtz Centre for Ocean Research Kiel, 24148 Kiel, Germany; orcid.org/0000-0003-3859-2112

Eric P. Achterberg – GEOMAR Helmholtz Centre for Ocean Research Kiel, 24148 Kiel, Germany; orcid.org/0000-0002-3061-2767

Complete contact information is available at:

<https://pubs.acs.org/10.1021/acsestwater.3c00096>

Notes

The authors declare no competing financial interest.

ACKNOWLEDGMENTS

Lesly Ayala Cabana and Vincent Fey performed early manual SPE tests that guided subsequent development described here. This work was financially supported by the ExPloTect project (co-funded by the European Maritime and Fisheries Fund, Project Number 863693). Research cruise ALS67 was funded by the Deutsche Forschungsgemeinschaft (DFG) through the GPF review process (Award GPF21-1_008 to J. Greinert). Additional support was provided by the GEOMAR Helmholtz Centre for Ocean Research Kiel and the Technik- und Logistik Zentrum (TLZ) at GEOMAR. The authors thank the two reviewers for their constructive comments on the manuscript.

REFERENCES

- (1) *Prevention of Marine Pollution by Dumping of Wastes and Other Matter (London Convention)* International Maritime Organization; 1972.
- (2) GICHD. *A Guide to Survey and Clearance of Underwater Explosive Ordnance*, 2016.
- (3) Pfeiffer, F. Changes in Properties of Explosives Due to Prolonged Seawater Exposure. *Mar. Technol. Soc. J.* **2012**, *46*, 102–110.
- (4) Beck, A. J.; Gledhill, M.; Schlosser, C.; Stamer, B.; Böttcher, C.; Sternheim, J.; Greinert, J.; Achterberg, E. P. Spread, Behavior, and Ecosystem Consequences of Conventional Munitions Compounds in Coastal Marine Waters. *Front. Mar. Sci.* **2018**, *5*, No. 141.
- (5) Appel, D.; Strehse, J. S.; Martin, H. J.; Maser, E. Bioaccumulation of 2,4,6-Trinitrotoluene (TNT) and Its Metabolites Leaking from Corroded Munition in Transplanted Blue Mussels (*M. Edulis*). *Mar. Pollut. Bull.* **2018**, *135*, 1072–1078.
- (6) Lotufo, G. R. Toxicity and Bioaccumulation of Munitions Constituents in Aquatic and Terrestrial Organisms. In *Challenges and*

- Advances in Computational Chemistry and Physics*; Springer, 2017; Vol. 25, pp 445–479.
- (7) Beck, A. J.; Gledhill, M.; Kampmeier, M.; Feng, C.; Schlosser, C.; Greinert, J.; Achterberg, E. P. Explosives Compounds from Sea-Dumped Relic Munitions Accumulate in Marine Biota. *Sci. Total Environ.* **2022**, 806, No. 151266.
- (8) Wolf, K. Dangerous Legacy. *Offshore Wind Ind.* **2017**, 3, 32–33.
- (9) Sayle, S.; Windeyer, T.; Charles, M.; Conrod, S.; Stephenson, M. Risk Assessment and Risk Management. *Mar. Technol. Soc. J.* **2009**, 43, 41–51.
- (10) Wang, P. F.; George, R. D.; Wild, W. J.; Liao, Q. *Defining Munition Constituent (MC) Source Terms in Aquatic Environments on DoD Ranges (ER-1453) SSC Pacific*; 2013.
- (11) U.S. EPA. *Method 8330B (SW-846): Nitroaromatics, Nitramines, and Nitrate Esters by High Performance Liquid Chromatography (HPLC)*, 2006.
- (12) Gledhill, M.; Beck, A. J.; Stamer, B.; Schlosser, C.; Achterberg, E. P. Quantification of Munition Compounds in the Marine Environment by Solid Phase Extraction – Ultra High Performance Liquid Chromatography with Detection by Electrospray Ionisation – Mass Spectrometry. *Talanta* **2019**, 200, 366–372.
- (13) Fu, X.; Benson, R. F.; Wang, J.; Fries, D. Remote Underwater Electrochemical Sensing System for Detecting Explosive Residues in the Field. *Sens. Actuators, B* **2005**, 106, 296–301.
- (14) Valkovic, V.; Sudac, D.; Matika, D.; Kollar, R. An Underwater System for Explosive Detection. In *Optics and Photonics in Global Homeland Security III*; SPIE, 2007.
- (15) Sharma, S. K. *Underwater Raman Sensor for Detecting High Explosives and Homemade Explosives (HMEs)*, ARL Winter 2016 Meeting, 2016.
- (16) Dock, M. L.; Harper, R. J.; Knobbe, E. Combined Pre-Concentration and Real-Time in-Situ Chemical Detection of Explosives in the Marine Environment. In *Ocean Sensing and Monitoring II*; SPIE, 2010.
- (17) Dasary, S. S. R.; Singh, A. K.; Senapati, D.; Yu, H.; Ray, P. C. Gold Nanoparticle Based Label-Free SERS Probe for Ultrasensitive and Selective Detection of Trinitrotoluene. *J. Am. Chem. Soc.* **2009**, 131, 13806–13812.
- (18) Ghosh, M.; Wang, L.; Asher, S. A. Deep-Ultraviolet Resonance Raman Excitation Profiles of NH₄NO₃, PETN, TNT, HMX, and RDX. *Appl. Spectrosc.* **2012**, 66, 1013–1021.
- (19) Jenkins, T. F.; Miyares, P. H.; Myers, K. F.; McCormick, E. F.; Strong, A. B. Comparison of Solid Phase Extraction with Salting-out Solvent Extraction for Preconcentration of Nitroaromatic and Nitramine Explosives from Water. *Anal. Chim. Acta* **1994**, 289, 69–78.
- (20) Greinert, J. *Practical Guide for Environmental Monitoring of Conventional Munitions in the Seas Results from the BMBF Funded Project UDEMM GEOMAR*; 2019.
- (21) Crockett, A. B.; Craig, H. D.; Jenkins, T. F. *Federal Facilities Forum Issue: Field Sampling and Selecting On-Site Analytical Methods For Explosives in Water* U.S. EPA; 1999.
- (22) Helms, J. R.; Stubbins, A.; Ritchie, J. D.; Minor, E. C.; Kieber, D. J.; Mopper, K. Absorption Spectral Slopes and Slope Ratios as Indicators of Molecular Weight, Source, and Photobleaching of Chromophoric Dissolved Organic Matter. *Limnol. Oceanogr.* **2008**, 53, 955–969.
- (23) Hansen, A. M.; Kraus, T. E. C.; Pellerin, B. A.; Fleck, J. A.; Downing, B. D.; Bergamaschi, B. A. Optical Properties of Dissolved Organic Matter (DOM): Effects of Biological and Photolytic Degradation. *Limnol. Oceanogr.* **2016**, 61, 1015–1032.
- (24) Haque, M. A. Feature Engineering & Selection for Explainable Models A Second Course for Data Scientists. <https://pypi.org/project/BaselineRemoval/> (accessed January 27, 2023).
- (25) Kampmeier, M.; van der Lee, E. M.; Wichert, U.; Greinert, J. Exploration of the Munition Dumpsite Kolberger Heide in Kiel Bay, Germany: Example for a Standardised Hydroacoustic and Optic Monitoring Approach. *Cont. Shelf Res.* **2020**, 198, No. 104108.
- (26) Gledhill, M.; Beck, A. J.; Stamer, B.; Schlosser, C.; Achterberg, E. P. Quantification of Munition Compounds in the Marine Environment by Solid Phase Extraction – Ultra High Performance Liquid Chromatography with Detection by Electrospray Ionisation – Mass Spectrometry. *Talanta* **2019**, 200, 366–372.
- (27) Beck, A. J.; van der Lee, E. M.; Eggert, A.; Stamer, B.; Gledhill, M.; Schlosser, C.; Achterberg, E. P. In Situ Measurements of Explosive Compound Dissolution Fluxes from Exposed Munition Material in the Baltic Sea. *Environ. Sci. Technol.* **2019**, 53, 5652–5660.
- (28) amucad.org. <https://amucad.org/map> (accessed January 27, 2023).
- (29) GEBCO Compilation Group, 2022. DOI: 10.5285/e0f0bb80-ab44-2739-e053-6c86abc0289c.